Reducing the CO_2 footprint at an LNG asset with replicate trains using operational data-driven analysis. A case study on end flash vessels.

Rakesh Paleja[a], Osemwinyen Ekhorutomwen[b], Matthew Jones[c], John Ayoola[b], Raghuraman Pitchumani[d], Philip Jonathan[a,e]

[a]*Shell Research Limited, London, United Kingdom.*
[b]*NLNG Plant Complex, Bonny Island, Rivers State, Nigeria*
[c]*Shell Global Solutions International BV, Amsterdam, The Netherlands.*
[d]*Shell International Exploration and Production Inc., Houston, Texas, USA.*
[e]*Department of Mathematics and Statistics, Lancaster University, United Kingdom.*

Abstract

A liquefied natural gas (LNG) facility often incorporates replicate liquefaction trains. The performance of equivalent units across trains, designed using common numerical models, might be expected to be similar. In this paper, we discuss statistical methods to validate this assumption. Analysis of operational data for end flash vessels from a pair of replicate trains at an African facility indicates that one train produces 2.8% to 6.4% more end flash gas than the other. We then develop statistical models for train operation, facilitating reduced flaring and hence a reduction in 45% in CO_2 emissions. We recommend that operational data-driven models be considered generally to improve the performance of LNG facilities and reduce their CO_2 footprint, particularly when replica units are present.

1. Introduction

Natural gas (NG) plays a significant role in the global energy transition, since switching from coal to NG reduces greenhouse gas emissions by 50% when producing electricity and 33% when providing heat; globally, up to 500 $MtCO_2$ were avoided in 2018 compared to 2010 (International Energy Agency, 2019). Natural gas sources in Australia, the Middle East, Russia, North America and Africa are often distant from consumer demand in Europe, Japan, South Korea, China and developing Asia (International Energy Agency, 2022). Transporting natural gas via pipeline over distances > 3000 km is not economically viable due to the low energy density of natural gas on a volumetric basis. Liquefaction of NG to $-163°C$ reduces its volume by a factor of around 600, permitting transportation by sea (Hafner and Luciani, 2022).

A large-scale LNG train typically consumes 4.5 to 6 kWh of energy per mole of LNG, with 40-60% of the energy used by compressors (Hasan et al., 2009a). The energy required is normally provided by fuel gas (FG) generated from different sources at the LNG producing facility including end flash gas (EFG) from end flash vessels, and boil off gas (BOG) from storage tanks and from loading vessels (LBOG). Economically and environmentally, it is advantageous to reduce demand for FG as much as possible consistent with demand, whilst avoiding flaring. This is achieved by process modelling using software such as AspenTech's HYSYS®, UniSim® and MATLAB®. For example in Alabdulkarem et al. (2011), minimization of compressor power in a C3MR process is performed through simulation in Aspen HYSYS ® and optimization in MATLAB ® using a genetic algorithm, leading to a 9% reduction in energy requirement. In Castillo et al. (2013), options to pre-cool NG using propane (C3) or ethane-propane (C2-C3) mixture-based pre-coolers are studied for hot and cold climate conditions using HYSYS® with a conclusion that C3 pre-cooling is the most energy efficient technology for both climates. In Hasan et al. (2009b), dynamic simulations are conducted to facilitate reducing in LBOG using "heel" as a parameter to be optimised; heel is the amount of LNG that is retained in the LNG vessel during its return journey to maintain the vessel as close as possible to -163 °C. Further, Jackson et al. (2017) modelled and optimised the energy requirement for a typical LNG train at different geographical locations and concluded that liquefaction in colder climates such as that of Norway would require 20-26% lower energy compared to warmer Australian or Middle Eastern climates. Compressors are thus proportionately smaller in colder countries.

Typically, multiple trains at a given LNG production facility have the same design. Multiple trains are preferred over a single large train for reasons such as (a) improved robustness of production to interruptions on an individual train, and (b) physical limitations on the design of a single large train. When multiple trains are operated at an LNG facility, some trains may be exact replicas of others in terms of liquefaction technology, size of compressors and other units such as end flash vessels. It would seem rational to expect that replicate trains offer some economies of scale.

Further, we might expect that performance of compressors and end flash vessel across the replicate trains would be similar; indeed, no further individual train-level optimisation is typically performed during train set-up. However, if replicated trains perform differently, there may be opportunities to further minimise energy consumption and flaring by comparing train performance using operational data.

Objectives and layout

In this paper, we use a two-step data-driven approach to demonstrate divergence in performance between two replicate trains at a full-scale LNG facility, focusing on comparison of end flash vessels at an African LNG facility. The first analysis step (reported in Section 3.1) involves exploratory analysis of historical data corresponding to multiple years of operation, to elucidate whether flash vessels from different trains produce different amounts of EFG under similar process conditions. Then we use statistical hypothesis testing (Section 3.2) to confirm significant divergence in EFG production between LNG trains. The second step (Section 4.1) involves the estimation of regression models for EFG production with respect to driver manipulable process variables. We demonstrate (Section 4.2) that these can be used to control excess EFG to minimise excess end flash gas and reduce CO_2 footprint. We emphasise that the two-step approach is not specific to any particular process unit or production technology. All that is required is a representative period of historical operational data for the near-replica production units.

Preceding the main analysis sections, Section 2 provides an overview of typical large-scale liquefaction. Following the analysis, Section 5 then provides discussion and conclusions. Summary statistics for flow rate from the two end flash vessels considered, and details of statistical hypothesis testing using Welch's t-test are relegated to Appendices Appendix A and Appendix B.

2. Description of LNG process

This section provides a brief overview of the components and operation of a liquefaction train, followed by a discussion of LNG facilities containing replicate trains and the potential this offers for improved operation.

2.1. The liquefaction train

A liquefaction train at an LNG facility is comprised of a hot and a cold section. NG from the gas field enters hot section, operating at above ambient temperature. Here, NG is pre-treated to remove acid gas (carbon dioxide and hydrogen sulphide), water and mercury. The processed NG then enters the cold section at temperature T1, pressure P1 and flow rate Q1 respectively as shown in Figure 1. Temperature T1 depends on the geographical location and can

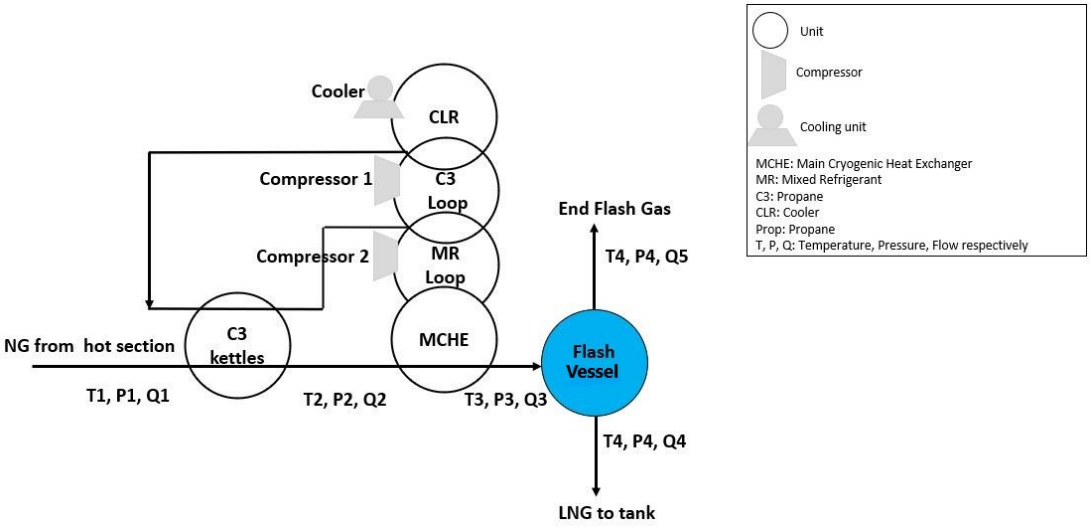

Figure 1: Schematic of cold section of LNG train. The end flash vessel shown in grey produces end flash gas, used as fuel gas for the facility.

vary from 25 to 30 °C, pressure P1 usually ranges from 50 to 60 bar whereas mass flow rate Q1 (tonnes/day, T/d) depends on the availability of NG. There are different designs for the cold section. In the C3MR design (Lim et al., 2012), the cold section pre-cools NG in C3 kettles from T1 to temperature T2 and subsequently to T3 in the main cryogenic heat exchanger (MCHE) using a mixer of refrigerants (MR). MR consists of liquid nitrogen (N2), C1, C2 and C3. T2 usually approaches -30 to -27 °C whereas T3 ranges from -150 to -145 °C depending on a variety of factors

such as NG composition, MR composition and pressure,and flow rates of NG and MR. The C3 kettles and MCHE are shell-and-tube heat exchanger units with NG flowing on the tube side, with liquid C3 (kettles) and liquid MR (MCHE) flowing on the shell side. The duty required to circulate propane and MR to cool NG from T1 to T3 is provided by two compressors. Figure 1 illustrates compressor 1 (C3) and compressor 2 (MR). Cooling NG from T1 to T3 results in vaporisation of C3 and MR; vapour heat is ejected to the atmosphere by air or water cooler before returning back to C3 kettles and MCHE respectively. When upstream pressure P1 is high, the final cooling to T4= $-163°$C occurs in the flash vessel, where NG from MCHE is flash evaporated at pressure P4 (close to the atmospheric pressure). As a result, the flow Q3 from the MCHE is divided into a vapour stream with flow rate Q5, and a liquid stream with flow rate Q4, the latter to storage tanks maintained at atmospheric pressure. The vapour stream is EFG to the FG pool, whereas the liquid stream is LNG for export. The nature of the flash evaporation process is such that $Q5 \ll Q4$ with $Q3 = Q4 + Q5$ to retain mass balance; the temperatures and pressures of the EFG and LNG are similar.

2.2. Replicate trains

As noted in Section 1, LNG facilities often contain replicate trains; Figure 2 shows a schematic for two replicate trains. Here, EFG from end flash vessels of each train is sent to the FG pool along with other sources of FG such as BOG and LBOG. The FG pool supplies the FG to the LNG facility. When there is excess FG, the flare valve is opened and the excess FG is flared. To prevent flaring, typical practice is to reduce EFG production from both trains equally, since trains are notionally replicates by design.

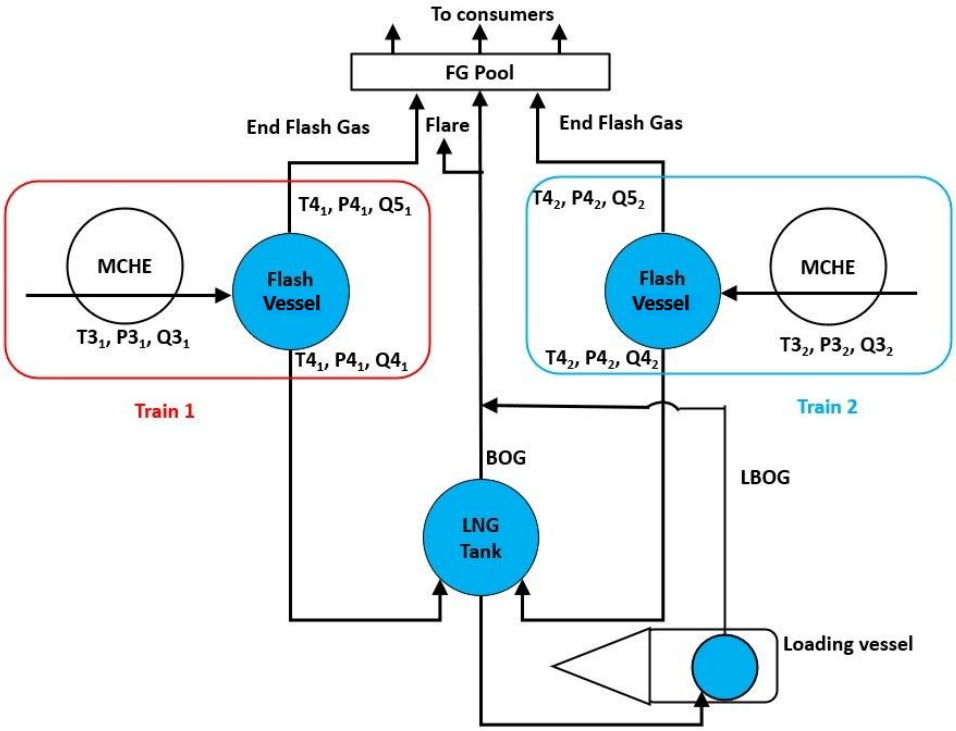

Figure 2: Schematic of two replicate trains, Train 1 and Train 2, feeding EFG to FG pool besides BOG from LNG tank LBOB from tank in the loading vessel (also shown in blue). When the FG pool has excess FG it is released and flared through the flare valve.

Table 1 shows LNG production from facilities with more than one train. It is likely that at least two trains at a facility are replicates of each other; while this information is not disclosed in the public domain, it is not unreasonable to assume this to be the case as such an approach reduces capital and operating expenditure. It is apparent that there is considerably potential to exploit operational data from replicate LNG trains to improve production efficiency.

3. Exploratory data analysis and hypothesis testing

In this section we present an analysis of operational data from an African LNG facility with two replicate liquefaction trains. The objective of the analysis is to identify differences in the operating characteristics of the two trains. The differences identified are then exploited in Section 4 to improve the overall performance of liquefaction, in particular with respect to reduced flaring of EFG. Section 3.1 provides an exploratory analysis of operational data, and Section 3.2 uses statistical hypothesis testing to demonstrate significant differences in operating characteristics for the trains.

LNG facility	Number of Trains	Capacity (million tonnes/annum) per train	all trains	Reference
Ras Laffan	2	3.3	-	
Ras Laffan (II)	3	4.7	-	
Ras Laffan 3	2	7.8	-	Qatar Gas (2023)
QatarGas 2	2	7.8	-	
Qatar Gas 1	3	3.3	-	
Nigeria LNG	6	-	22	Nigeria LNG (2023)
Oman LNG	3	-	-	Oman LNG (2023)
Brunei LNG	5	-	6.71	Wikipedia:Brunei LNG (2023)
Wheatstone LNG	2	4.3	-	Wikipedia:Wheatstone LNG (2023)
Gladstone LNG	2	-	-	Wikipedia:Gladstone LNG (2023)
Gorgon LNG	3	5.2	-	Wikipedia:Gorgon LNG (2023)
Sakhalin 2	2	4.8	-	Wikipedia:Sakhalin II LNG (2023)
Yamal LNG	3	-	16.5	Wikipedia:Yamal LNG (2023)

Table 1: LNG production data for select facilities.

We emphasise that the analysis is intended to exploit different operating characteristics of notionally replicate LNG trains. A necessary preliminary step therefore is to ensure that trains considered are indeed replicates. We have confirmed this for a pair of trains, henceforth identified as Tr_1 and Tr_2, from the African facility.

3.1. Exploratory analysis

We consider the operation of flash vessel units U_1, U_2 of replicate trains Tr_1, Tr_2, with EFG mass flow rates $\mathrm{Q5}_1$, $\mathrm{Q5}_2$. Figure 1 motivates the assumption that Q5 for individual units is dependent on (a) the corresponding flow Q3 of NG from the MCHE to the flash vessel, (b) the outlet temperature T3 of NG from the MCHE to the flash vessel, and (c) flash vessel pressure P4. The "manipulated" (or, in statistical terminology, "treatment") variables Q3, T3, P4 can be changed independently, thereby influencing Q5. We anticipate that increasing the values of Q3 and T3 will lead to a higher value of Q5. Conversely a higher P4 will lead to lower Q5.

We seek to assess fairly whether Q5 from U_1 and U_2 is similar. Ideally, we would conduct a series of experiments on both units, where the values of Q3, T3 and P4 were set at common values across trains, and differences in Q5 quantified. However, such experiments are impractical economically for trains in continuous operation. Nevertheless, over the course of normal operation of the trains in time, the set points of Q3, T3 and P4 for the two trains vary, exploring a domain of typical set points for both trains. We can therefore exploit these historical data to quantify differences in Q5. It is of course critical that our assessment is fair, in particular because the domains of Q3, T3 and P4 might be different for the two trains. Since Q5 depends on Q3,T3 and P4, it is essential that the historical data for both the trains is filtered such that the treatment variables Q3, T3 and P4 correspond to similar sets of values across the two units. Concisely in mathematical notation, we wish to compare Q5|(Q3,T3,P4) conditionally across trains, rather than Q5 marginally. The simple filter condition applied takes the form

$$\mathrm{LL} <= X_1^t/X_2^t <= \mathrm{UL} \quad \text{for all of } X = \mathrm{Q3},\ \mathrm{T3},\ \mathrm{P4} \tag{1}$$

where X^t is the value of X and time t, for data sampled every 5 minutes for a period of a contiguous calendar year. We emphasise that the filter considered is applied to all of X = Q3, T3 and P4. Further, LL indicates a common lower limit for the ratio of manipulated variables across trains, set at 0.98 in this work. UL indicates the corresponding common upper limit, set at 1.02. The effect of filtering manipulated variables is illustrated in Figure 3. Panels of the figure are scatter plots of X_2 on X_1 for X = Q3, T3, P4 and Q5, with green dots indicating data for time points at which the filter conditions in Equation 1 are satisfied. Data for all other time points is shown in blue. Of course, filtering yields subsets of operational data for Tr_1 and Tr_2 of equal size. For reasons of commercial confidentiality, note also that all flows Q3 and Q5 presented in this work (e.g. in Figure 3, Figure 4 and accompanying tables in Appendix Appendix A) have been normalised using a common factor k (i.e. Normalised Flow = $k \times$ Observed Flow) such that the maximum Q5 (over all trains and years) in the filtered data is 100 T/d after normalisation. No other variables are normalised.

The quality of NG sourced from upstream wells, distributed to the two trains, varies over time. As the proportion of low boiling point components (e.g. C2, C3, and butane, C4) in NG increases, Q5 production reduces in both U_1 ad U_2. Moreover, the performance of LNG trains often exhibits seasonal patterns that can influence Q5; filtering (Equation 1) ensures that the comparison of units is not influenced by season and other external variation of the common NG input

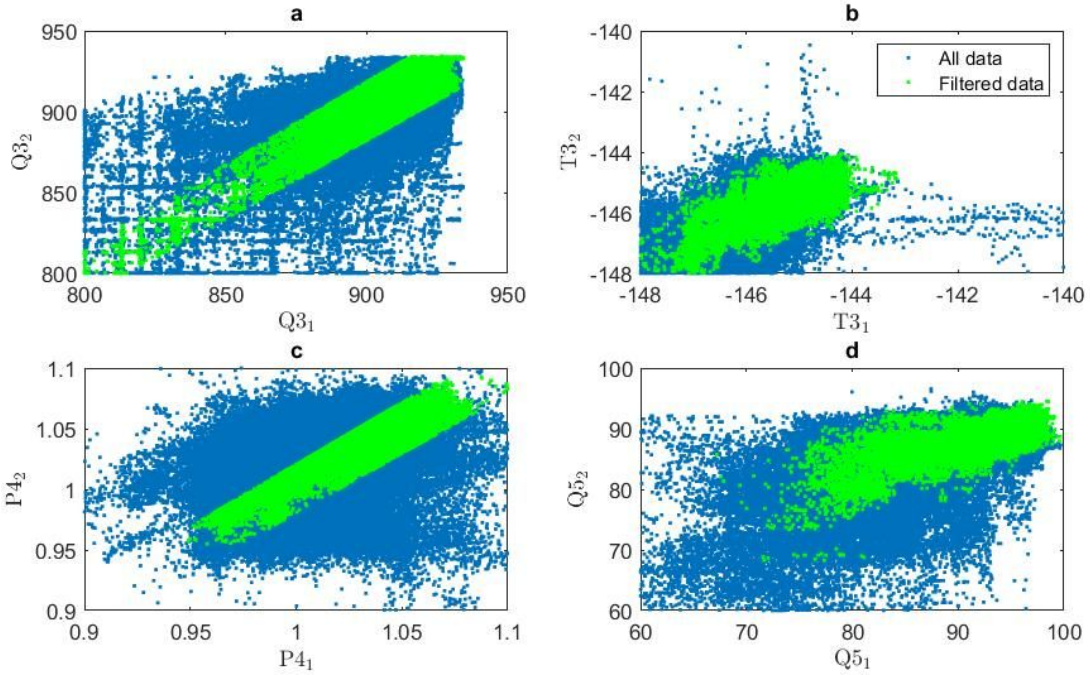

Figure 3: Scatter plots of Q3, T3, P4 and Q5 across trains Tr_1, Tr_2 for one year of operational data sampled at 5 minute intervals. Values for time points satisfying the filter conditions in Equation 1 are shown in green. All other time points are shown in blue. Values of Q3 and Q5 have been normalised using a common factor so that the global maximum value of Q5 is 100 T/d.

to liquefaction. Filtering therefore allows us to characterise underlying differences in the operational characteristics of the trains, rather than differences in inputs and operating set points.

Since (replicate) trains are optimised through numerical simulations during design, we expect differences in Q5 across trains to to be small. We might therefore expect that a comparatively long period of historical data might be required to quantify differences in operational characteristics with confidence: in particular, analysis of filtered data from only one year can lead to spurious conclusions. Therefore here, we analyse historical operational data for the five year period 2015 to 2019. The panels of Figure 4 shows histograms of filtered Q5 per annum for years 2015 to 2019, for train Tr_1 (blue) and Tr_2 (red). The title of each plot shows the year and number n of filtered 5-minute observations. Vertical blue and red lines and annotated text give sample means of filtered $\mathrm{Q5}_1$ and $\mathrm{Q5}_2$ respectively. Figure 4 suggests for each of the five years, that Q5 through U_1 is greater than that through U_2. The difference in sample means ranges from 2.5 to 5.5 T/d. Corresponding tables of summary statistics are provided in Appendix Appendix A. It is also interesting that the number of observations retained after filtering is considerably higher in 2018 and 2019 that 2016 in particular, possibly indicating more consistent setting of operational conditions across trains in more recent years.

The figure for unfiltered data corresponding to Figure 4 is show in Figure 5. It is notably difficult to see from the figure that there is a material difference between the operating characteristics of trains Tr_1 and Tr_2. This emphasises the need to consider the conditional behaviour of Q5 given its driver variables Q3, T3, P4.

3.2. Statistical testing

The exploratory analysis above suggests that Q5 from vessel U_1 in train Tr_1 is higher than that from U_2 in train Tr_2. We can quantify this using a statistical hypothesis test to assess whether the population mean $\overline{\mathrm{Q5}}_1$ of Q5 in train Tr_1 is greater than the corresponding population mean $\overline{\mathrm{Q5}}_2$ in train Tr_2. To perform this one-sided hypothesis test, we set the null hypothesis H_0 that there is no difference between $\overline{\mathrm{Q5}}_1$ and $\overline{\mathrm{Q5}}_2$, and an alternative hypothesis H_1 that $\overline{\mathrm{Q5}}_1 > \overline{\mathrm{Q5}}_2$. Then we calculate whether there is sufficient evidence in the data to reject the null hypothesis in favour of the alternative. Various parametric and non parametric tests are suggested in the literature (e.g. Marshall and Jonker 2011) for this purpose. The choice of test depends on the nature of the data and the specific question at hand. Here we use the independent two-sample Student's t-test, calculating test-statistic t measuring the difference in population means relative to the variability within the groups using sample data. This test assumes that the variances of the two samples are approximately equal. For samples of random variables X_1 and X_2 with common sample size n, t is calculated as

$$t = (\bar{X}_1 - \bar{X}_2)/s_d \tag{2}$$

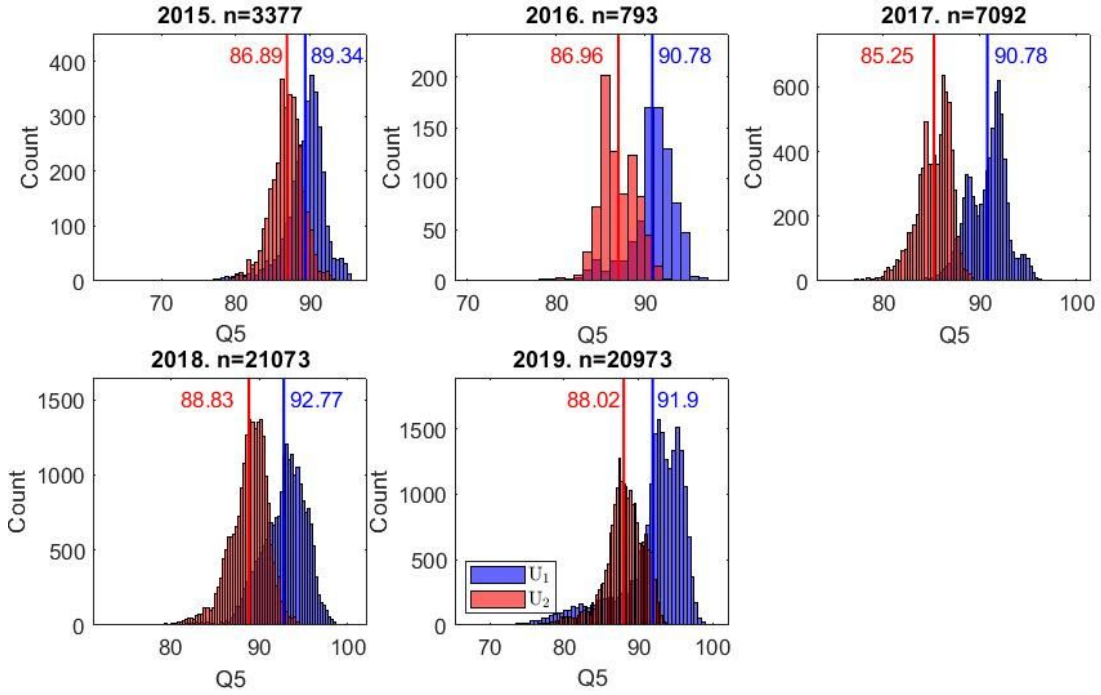

Figure 4: Histograms of filtered $Q5_1$ (blue) and $Q5_2$ (red) data per annum, for years 2015 to 2019. Panel titles indicate the number of observations n retained after filtering. Vertical lines and annotated text give mean values of filtered data. Values of Q5 have been normalised using a common factor so that the global maximum value is 100 T/d.

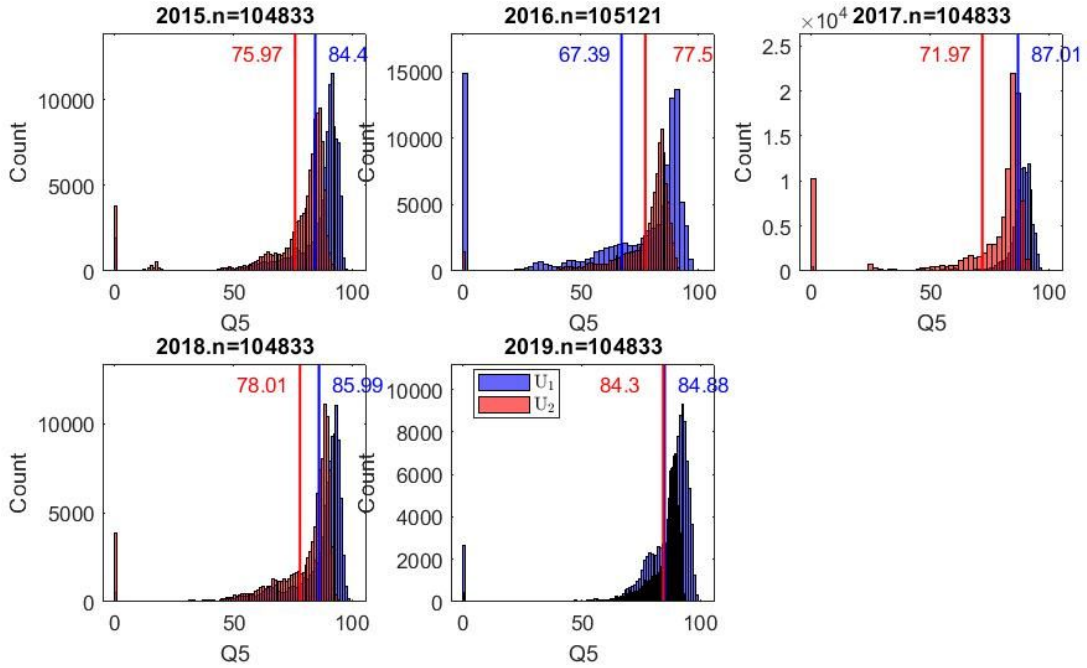

Figure 5: Histograms of full unfiltered data for $Q5_1$ (blue) and $Q5_2$ (red) per annum, for years 2015 to 2019. Panel titles indicate the number of observations n retained after filtering. Vertical lines and annotated text give mean values of filtered data. Values of Q5 have been normalised using a common factor so that the global maximum value is 100 T/d.

where $\bar{X}_1$ and $\bar{X}_2$ are the sample means for $Q5_1$ and $Q5_2$ (from Tables A.1 and A.2 in Appendix A), and s_d is the standard error of the difference in means given by $s_d^2 = (s_1^2 + s_2^2)/n$, where s_1^2 and s_2^2 are corrected sample estimates for the variance of X_1 and X_2. s_d can also be written as $s_d^2 = 2s_p^2/n$, where s_p is an estimate for the pooled standard deviation of the samples given by $s_p^2 = (s_1^2 + s_2^2)/2$. The test statistic t follows a t-distribution with $\nu = 2(n-1)$ degrees of freedom (Evans et al., 2000). This probability distribution generalizes the standard normal distribution:

both the t-distribution and standard normal distribution have mean zero and exhibit a bell-shaped curve, but the t-distribution has heavier tails controlled by shape parameter ν. Typically, the null hypothesis H_0 is rejected at the $\alpha = 0.05$ level; this occurs when the value of the t-statistic calculated exceeds a critical value $t_{\text{crit},\nu}(1-\alpha)$ equal to the $(1-\alpha)\times 100 = 95\%$ile of the t-distribution with ν degrees of freedom.

$$(\bar{X}_1 - \bar{X}_2)/s_d - t_{\text{crit},\nu}(0.95) > 0. \tag{3}$$

Multiplying the left hand side above by s_d gives $(\bar{X}_1 - \bar{X}_2) - s_d \times t_{\text{crit},\nu}(0.95)$, equal to the lower confidence limit LCL for the difference $\bar{X}_1 - \bar{X}_2$ in population means. Rejecting H_0 is therefore also equivalent to estimating LCL¿0. For total sample $n > 100$, $t_{\text{crit},2(n-1)}(0.95) \approx 1.645$, the 95%ile of standard normal distribution, to at least two decimal places; for smaller sample sizes, values of $t_{\text{crit},2(n-1)}(0.95)$ are provided by standard statistical software.

Table 2 shows the results of significance testing for the difference in population mean duty, $\overline{\text{Q5}}_1$ - $\overline{\text{Q5}}_2$, between trains Tr_1 and Tr_2, annually from 2015 to 2019. In percentage terms, $\overline{\text{Q5}}_1$ exceeds $\overline{\text{Q5}}_2$ by some 2.8% to 6.4%.

Year	2015	2016	2017	2018	2019
$\overline{\text{Q5}}_1$ - $\overline{\text{Q5}}_2$	2.450	3.816	5.531	3.948	3.885
s_p	2.458	2.489	1.926	2.417	3.729
s_d	0.0598	0.1250	0.0324	0.0236	0.0364
$\nu = 2(n-1)$	6752	1584	14182	42144	41944
$t_{\text{crit},\nu}(0.95)$	1.645	1.645	1.645	1.645	1.645
LCL	2.333	3.571	5.467	3.902	3.814

Table 2: Independent two-sample t-test for population mean difference $\overline{\text{Q5}}_1$ - $\overline{\text{Q5}}_2$ per annum. Null hypothesis rejected for each year since LCL¿0.

When there is evidence that the variance of the two samples is not equal, we can use the Welch's t-test (Welch 1947) as an alternative to the test above. For the current data, using the corresponding Welch test at $\alpha = 0.05$, the null hypothesis of equality of $\overline{\text{Q5}}_1$ and $\overline{\text{Q5}}_2$ was also reject for each of the years 2015 to 2019; see Appendix Appendix B for details.

4. Regression analysis to reduce excess fuel gas to flare

When the supply of FG is greater than the demand for it, excess FG is flared. FG supply sources are LBOG, BOG and two Q5 streams. Since there is no control on BOG or LBOG contributing to the FG pool, reducing Q5 for the two trains is the only mechanism to reduce excess FG and prevent flaring. Since the trains are assumed due to common design to be replicates, it is typically assumed that common manipulation of process variables influencing Q5 is the wisest course of action. However, in Section 3, clear differences in the operational characteristics of trains Tr_1 and Tr_2 were identified. In this section, we exploit those differences to improve process performance, and in particular to reduce the need for flaring, by manipulating the replicate trains differently at the onset of flaring events.

4.1. Regression and adjusted regression plots

For each of units U_1 and U_2 on trains Tr_1 and Tr_2 respectively in turn, we establish linear regression models for Q5 in terms of Q3, T3 and P4 of the form

$$\text{Q5} \quad = \quad f(\text{Q3}, \text{T3}, \text{P4}) + \epsilon \tag{4}$$

for regression function f, where ϵ is assumed to be a zero-mean Gaussian random variable with unknown standard deviation. Here, we assume that f takes the linear form

$$f(\text{Q3}, \text{T3}, \text{P4}) = a + b\ \text{Q3} + c\ \text{T3} + d\ \text{P4} \tag{5}$$

for parameters a, b, c and d to be estimated. Following DuMouchel (1988), we then use adjusted response or adjusted regression plots to quantify the effects of individual treatment variables (more naturally referred to as covariates in a regression context) in regression models for Q5 in terms of Q3, T3 and P4, for each of trains Tr_1 and Tr_2. In essence, these are generalisations of partial residual and augmented partial residual plots (Mallows 1986), useful for linear regression models with arbitrary power and interaction terms. The fitted regression function $\hat{f}$ from Equation 4 is

$$\hat{f}(\text{Q3}, \text{T3}, \text{P4}) = \hat{a} + \hat{b}\ \text{Q3} + \hat{c}\ \text{T3} + \hat{d}\ \text{P4}$$

where $\hat{\bullet}$ represents an estimate. The corresponding residuals from the regression form the set $\{r^i\}_{i=1}^n$, with

$$r^i = Q5^i - \hat{f}(\mathrm{Q3}^i, \mathrm{T3}^i, \mathrm{P4}^i) \quad \text{for } i = 1, 2, ..., \mathrm{n}$$

where $\{\mathrm{Q3}^i, \mathrm{T3}^i, \mathrm{P4}^i\}_{i=1}^{\mathrm{n}}$ is the set of values of Q3, T3 and P4 in the data sample of filtered data for regression model fitting.

Next, adjusted fit functions are calculated for each of Q3, T3 and P4 in turn. For example in the case of Q3, the adjust fit function is the average value of $\hat{f}$, expressed as a function of Q3, over all n observations in the data sample

$$g_{Q3}(q) = \frac{1}{n}\sum_{i=1}^{n} \hat{f}(q, \mathrm{T3}^i, \mathrm{P4}^i).$$

Similar adjusted fit functions can be derived for each covariate in each train in turn. Finally the set $\{\tilde{Q5}_{Q3}^i\}_{i=1}^n$ of adjusted response values for Q5 with respect to Q3 is calculated using

$$\tilde{Q5}_{Q3}^i = g_{Q3}(\mathrm{Q3}^i) + r^i \quad \text{for } i = 1, 2, ..., \mathrm{n}$$

where $\{r^i\}_{i=1}^n$ are the residuals from the full regression (Equation 4). Similar sets of adjusted response values can be calculated for response Q5 with respect to each covariate in each train in turn.

Adjusted response values for Q5 with respect to each of Q3, T3 and P4 are shown in Figure 6, for train Tr_1 (blue) and Tr_2 (red). The anticipated directions of the trends of Q5 with covariates are seen in each case. However, despite the trains being nominally replicates, the magnitudes of gradients are larger for train Tr_1 regardless of covariate. Briefly, Q5 is more sensitive to changes in covariates for train Tr_1. To achieve unit reduction in Q5, the reduction in

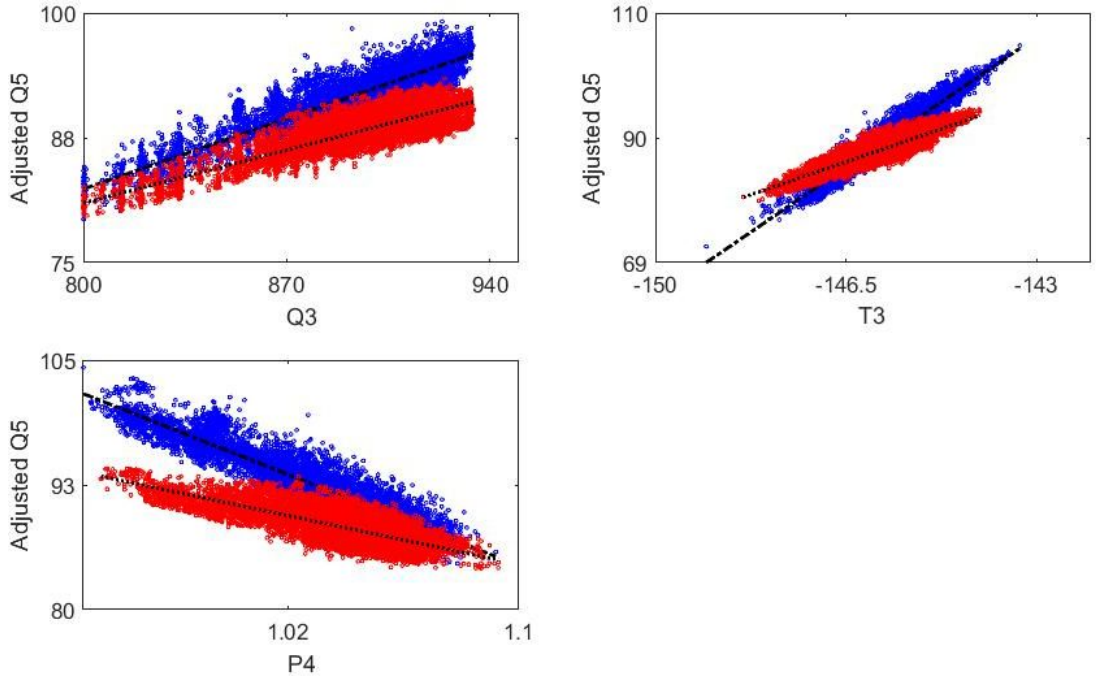

Figure 6: Adjusted response values for Q5 with respect to Q3, T3 and P4 for U_1 (blue circles) and U_2 (red circles). Corresponding adjusted fit functions g are shown as black lines.

Q3 (and/or T3) needed in Tr_1 is smaller than that needed in Tr_2. This is potentially a valuable handle with which to reduce the need for flaring.

Note that the adjusted regression methodology is applicable generally, regardless of the form of the regression function in Equation 4.

4.2. Implementation of recommendations

Given the findings above, trials were conducted on the liquefaction trains to evaluate the impact on flaring of different manipulations of set-points of manipulated variables on Tr_1 and Tr_2 end flash units U_1 and U_2. In a first period ("Period 1"), each time the flare valve was on the verge of opening, a common reduction of T3 was made

for both trains, followed by common reduction of Q3 if necessary. In the second period ("Period 2"), preferential treatment was given to Tr_1: $T3_1$ was reduces first, followed if necessary by $Q3_1$, $T3_2$ and $Q3_2$ if flaring persisted. P4 was not used as a handle during the trial. Results are shown in Figure 7. Panels show the mean flare valve opening

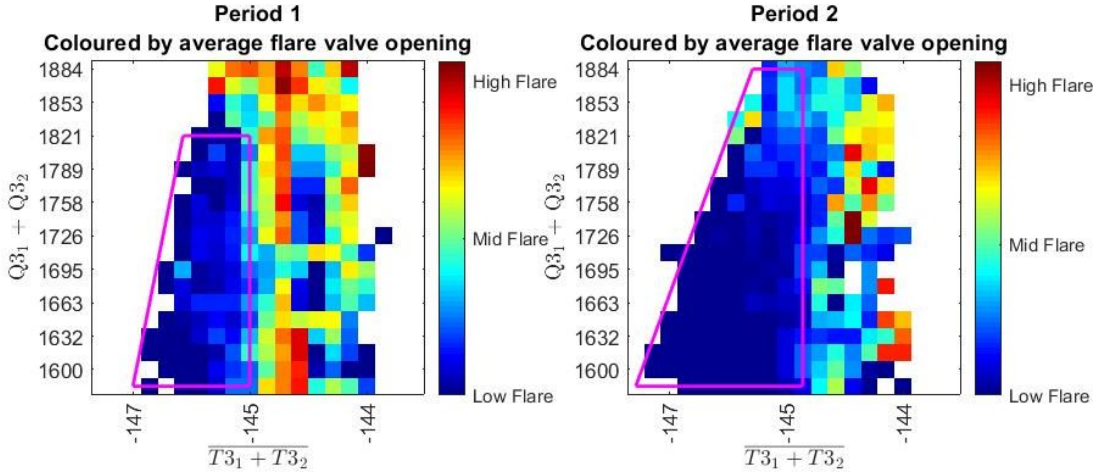

Figure 7: Flare valve opening, ranging from High, Medium to Low for Period 1 (left) and Period 2 (right) as a function of mean of T3 and sum of Q3 from Tr_1 and Tr_2 . In Period 1, simultaneous and equal reductions were made, first for T3 and subsequently if necessary for Q3, for both trains at the point of flare onset. In Period 2, $T3_1$ and then $Q3_1$ (if necessary) were reduced first, followed (if necessary) by $T3_2$ and $Q3_2$. Polygons shows domains of mean T3 and total Q3 corresponding to low risk of High and Medium flare opening.

in Periods 1 (left) and 2 (right) as a function of the mean T3 (x-axis) and total Q3 (y-axis). The figure indicates a reduction in High and Medium flare valve opening in Period 2 compared to Period 1 of approximately 45%. Polygons (magenta) in each panel show approximate approximate ranges for mean T3 and total Q3 within which the risk of High or Medium flaring is low. The area of the polygon for Period 2 is considerably wider than for Period 1, indicating that reduction of T3 and Q3 for Tr_1 before those of Tr_2 is advantageous in reducing FG flaring.

5. Discussion and conclusions

This article demonstrates that differences in the operating characteristics of nominally replicate units at an LNG facility can be exploited to improve the overall performance of the facility, in particular by minimising flaring. We demonstrate that careful exploratory analysis can be used to identify differences in operating characteristics, and that statistical hypothesis testing lends weight to findings from exploratory work. We then show that simple regression models can be used to illustrate and quantify differences in unit performance. Finally, we demonstrate by modifying operating practices at the "live" LNG facility, that the recommendations of the statistical analysis provide clear material benefit.

The statistical analysis conducted here is elementary but sound. Indeed, we hope the current work demonstrates the real-world benefits available from careful application of straightforward statistical thinking and method: complicated models are not always necessary for process improvement in manufacturing. Nevertheless, there are numerous ways in which the current analysis can be improved. For example, preliminary analysis suggests there may some benefit from consideration of seasonal trends in the relative operating characteristics of the flash vessel units.

Specifically, our study of end flash vessels from two trains at an African LNG facility has shown that statistically significant differences in train performance can exist even though trains may be "exact copies" of each other from a design perspective. The flow rate of end flash gas (EFG, Q5) produced from one end flash vessel is found to be 2.8% to 6.4% higher than from the other replicate unit. As a result, on the onset of EFG flaring, the standard practice of reducing natural gas input temperature (T3) and flow rate (Q3) simultaneously and equally to the main cryogenic heat exchangers of the two trains to minimise flaring is demonstrably not best practice. An improved procedure based on the current statistical analysis first reduces T3 and Q3 for the train whose EFG production is more sensitive to operating conditions. When this strategy was followed at the LNG facility, flaring was reduced by 45% compared with standard practice.

Insights from analysis of operational data cannot be obtained from simulation studies of model trains with identical designs. We hope the current paper serves as motivation for wider use of data-informed and data-driven approaches for improved efficiency in manufacturing.

6. Acknowledgement

We acknowledge the support of colleagues at Shell during the execution of this project, and publication of this article.

Appendix A. Appendix: Annual summary statistics for Q5 from trains $\mathbf{Tr_1}$, $\mathbf{Tr_2}$ for years 2015-2019

This appendix gives summary statistics for normalised filtered Q5 from trains Tr_1, Tr_2 for years 2015-2019, corresponding to Figure 4. These values are also used in the statistical testing reported in Section 3.

Year	Mean	Median	Variance s^2	Skewness	Kurtosis
2015	89.34	89.80	7.22	-1.17	5.69
2016	90.78	91.15	8.30	-1.95	10.03
2017	90.78	91.15	4.13	-0.38	3.56
2018	92.77	93.13	6.84	-1.08	6.34
2019	91.90	92.99	20.08	-1.54	5.26

Table A.1: Summary statistics of samples of filtered Q5 values for train Tr_1 over years 2015 to 2019. Values have been normalised using a common factor so that the global maximum value (over both trains and all years) is 100 T/d.

Year	Mean	Median	Variance	Skewness	Kurtosis
2015	86.89	87.02	4.86	-0.86	8.29
2016	86.96	86.58	4.09	0.15	2.67
2017	85.25	85.54	3.30	-0.91	4.34
2018	88.83	89.11	4.85	-0.87	4.91
2019	88.02	88.19	7.74	-1.28	6.93

Table A.2: Summary statistics of filtered Q5 values for train Tr_2 over years 2015 to 2019. Values have been normalised using a common factor so that the global maximum value (over both trains and all years) is 100 T/d.

Appendix B. Appendix: One-tailed, two-sample Welch's t-test for un-equal variance

In the notation of Section 3.2, the expression for Welch's t-test statistic (Welch 1947) to compare the means of populations with unequal population variances of X_1 and X_2, but equal sample size n, is the same as that given in Equation 2. The degrees of freedom ν of the t-distribution is however different, given by Satterthwaite's approximation (Satterthwaite, 1946) as

$$\nu = \frac{(n-1)(s_1^2 + s_2^2)^2}{s_1^4 + s_2^4}$$

where s_1 and s_2 are the corrected sample standard deviations for the two groups; the Welch's t-test is more conservative in estimating ν. The corresponding table of results using Welch's t-test is given in Table (c.f. Table 2) is given in Table B1.

Year	2015	2016	2017	2018	2019
$\overline{\mathrm{Q5}}_1$ - $\overline{\mathrm{Q5}}_2$	2.450	3.816	5.530	3.948	3.885
ν	6504.9	1419.7	14007	40953	35055
$t_{\mathrm{crit},\nu}(0.95)$	1.9603	1.9615	1.9601	1.96	1.96
LCL	2.333	3.571	5.467	3.901	3.814

Table B1: Welch's t-test for population mean difference $\overline{\mathrm{Q5}}_1$ - $\overline{\mathrm{Q5}}_2$ per annum, assuming unequal population variances. Null hypothesis rejected for each year since LCL¿0.

References

Alabdulkarem, A., Mortazavi, A., Hwang, Y., Radermacher, R., Rogers, P., 2011. Current status and perspectives of liquefied natural gas (lng) plant design. Applied Thermal Engineering 31, 1091–1098.

Castillo, L., Dahouk, M.M., Scipio, S.D., Dorao, C., 2013. Conceptual analysis of the precooling stage for LNG processes. Energy Conversion and Management 66, 41–47.

DuMouchel, W., 1988. Graphical representations of main effects and interaction effects in a polynomial regression on several predictors, in: DTIC ADA208838: Computing Science and Statistics: Proceedings of the 20th Symposium on the Interface: Computationally Intensive Methods in Statistics (Fairfax, Virginia), pp. 127–132.

Evans, M., Hastings, N., Peacock, B., 2000. Statistical Distributions. Wiley.

Hafner, M., Luciani, G. (Eds.), 2022. The Palgrave Handbook of International Energy Economics. URL: https://link.springer.com/chapter/10.1007/978-3-030-86884-0_2.

Hasan, M., Karimi, I., Alfadala, H., 2009a. Optimizing compressor operations in an LNG plant. Proceedings of the 1st Annual Gas Processing Symposium 48, 179–184.

Hasan, M.M.F., Zheng, A.M., Karim, I.A., 2009b. Minimizing boil-off losses in liquefied natural gas transportation. Ind. Eng. Chem 48, 9571–9580.

International Energy Agency, 2019. The role of gas in today's energy transitions. URL: https://iea.blob.core.windows.net/assets/cc35f20f-7a94-44dc-a750-41c117517e93/TheRoleofGas.pdf.

International Energy Agency, 2022. World energy outlook. URL: https://iea.blob.core.windows.net/assets/830fe099-5530-48f2-a7c1-11f35d510983/WorldEnergyOutlook2022.pdf.

Jackson, S., Eiksund, O., Broda, E., 2017. Impact of ambient temperature on LNG liquefaction process performance: Energy efficiency and co2 emissions in cold climates. Industrial and Engineering Chemical Research 56, 3388–3398.

Lim, W., Choi, K., Moon, I., 2012. Current status and perspectives of liquefied natural gas (LNG) plant design. Industrial and Engineering Chemistry Research 52, 3056–3088.

Mallows, C.L., 1986. Augmented partial residuals. Technometrics 28, 313–319.

Marshall, G., Jonker, L., 2011. An introduction to inferential statistics: A review and practical guide. Radiography 17, 1–6.

Nigeria LNG, 2023. The plant. URL: https://www.nigerialng.com/operations-strategies/Pages/The-Plant.aspx.

Oman LNG, 2023. Process of liquefaction. URL: https://omanlng.co.om/en/Pages/process-of-liquefaction.aspx.

Qatar Gas, 2023. Qatar gas portfolio. URL: https://www.qatargas.com/english/aboutus/Documents/Venture/Portfolio_Final.pdf.

Satterthwaite, F., 1946. An approximate distribution of estimates of variance components. Biometrics Bulletin 2, 110–14.

Welch, B.L., 1947. The generalisation of "student's" problem when several different population variances are involved. Biometrika 34, 28–35.

Wikipedia:Brunei LNG, 2023. Brunei lng. URL: https://en.wikipedia.org/wiki/Brunei_LNG.

Wikipedia:Gladstone LNG, 2023. Gladstone LNG. URL: https://en.wikipedia.org/wiki/Gladstone_LNG.

Wikipedia:Gorgon LNG, 2023. Gorgon LNG. URL: https://en.wikipedia.org/wiki/Gorgon_gas_project.

Wikipedia:Sakhalin II LNG, 2023. Sakhalin LNG. URL: https://en.wikipedia.org/wiki/Sakhalin-II.

Wikipedia:Wheatstone LNG, 2023. Wheatstone LNG. URL: https://en.wikipedia.org/wiki/Wheatstone_LNG.

Wikipedia:Yamal LNG, 2023. Yamal LNG. URL: https://en.wikipedia.org/wiki/Yamal_LNG.